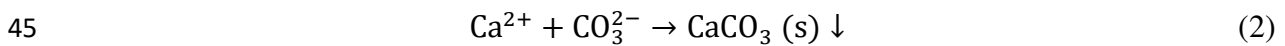
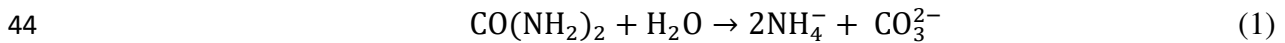


27 **Author Keywords:** Microbially induced calcite precipitation (MICP); bio-cemented sand;
28 ground improvement; microstructural analysis; unconfined compressive strength (UCS).

29 **Introduction**

30 Due to its versatility and sustainable application, microbially induced calcite precipitation
31 (MICP) has recently gained much attention from the geotechnical engineering researchers
32 worldwide. MICP is a naturally driven biological technique that harnesses the metabolism of
33 bacteria to create an in-situ cementation agent known as calcium carbonate or calcite.
34 Although there are many biological processes that can lead to MICP, the use of urea
35 hydrolysis by ureolytic bacteria is gaining more interest, and the current study will thus focus
36 on MICP via urea hydrolysis pathway. In this technique, aerobically cultivated bacteria with
37 highly active urease enzyme (*Sporosarcina pasteurii*, formerly known as *Bacillus pasteurii*)
38 are introduced to a targeted soil. The urea hydrolysis takes place when the active ureolytic
39 bacteria catalyze the reaction of urea hydrolysis to produce ammonium (NH₄⁺) and carbonate
40 ions (CO₃²⁻). In the presence of calcium from a supplied calcium source (i.e. CaCl₂), crystals
41 of calcium carbonate (i.e. calcite) form inside the soil matrix. The chemical reactions
42 involved in this technique are as follows:

43



46

47 The bonding of soil particles by calcite provides an improvement to the mechanical and
48 geotechnical engineering properties of bio-treated soils (DeJong et al. 2010). For example,
49 bio-cemented sand treated by MICP has been reported to provide a reduction in soil
50 settlement (DeJong et al. 2006; van Paassen et al. 2010a), an increase in soil shear strength
51 (Ismail et al. 2002a; DeJong et al. 2006; Chou et al. 2011), and an improvement in soil
52 stiffness (Montoya and DeJong 2015; Feng and Montoya 2015; Lin et al. 2015). In an attempt
53 to advance the MICP technique for field implementation, van Paassen et al. (2010b) applied
54 MICP to treat 100 m³ of sand in a large-scale experiment, and the results demonstrated that

55 MICP was able to improve large spatial areas of treated sand. DeJong et al. (2014) developed
56 a repeated five-spot treatment model to simulate a more realistic soil volume treatment in the
57 field, and it was found that the proposed model was able to show spatial and temporal trends
58 in the microbial content, which indicates that the model has the means to capture the complex
59 treatment scenario involving MICP.

60

61 Mortensen et al. (2011) studied the environmental factors affecting MICP, namely the
62 aqueous environmental conditions, various soil particle sizes and soil gradation. The results
63 showed that the natural aqueous environments (freshwater and seawater) and myriad soil
64 particle sizes and gradation (gravel, well-graded sand, poorly-graded sand and silt) were
65 equally favorable to calcite precipitation. Mortensen et al. (2011) also proposed that the
66 calcite precipitation rate and nutrient concentrations must be kept to their minimum in order
67 to achieve treatment homogeneity across the bio-cemented soil columns. Similar findings
68 were reported by Al Qabany and Soga (2013). However, the correlation between the
69 mechanical and geotechnical behavior and amount of calcite formed under the above
70 conditions has not been yet investigated. Earlier studies on the correlation between the shear
71 strength of bio-cemented sand and amount of calcite content enveloping the sand particles
72 have been investigated by Fujita et al. (2000) and Okwadha and Li (2010), showing that the
73 shear strength of sand may not be directly proportional to the amount of calcite content
74 (Whiffin et al. 2007). This was confirmed and explained by Cheng et al. (2013) who observed
75 deposition of calcite crystals in the contact points between the sand grains, forming effective
76 bridges that contribute to the shear strength improvement of bio-cemented soil.

77

78 The calcite precipitation pattern is another factor that greatly influences the target application
79 of bio-cementation in the field as it influences the flow properties of porous media, which
80 may lead to treatment homogeneity by shaping the preferential flow path according to the

81 size, shape, and structure of the pore throats affected by the accumulation of calcite crystals
82 (Al Qabany et al. 2012). The calcite precipitation pattern also affects the load transfer
83 mechanism between the soil particles, through the area of contact points developed by the
84 precipitated calcite, leading to variation in strength and stiffness of bio-cemented soils (Ismail
85 et al. 2002b).

86

87 This paper aims to investigate the impact of some key environmental parameters on the
88 efficacy of MICP for its in-situ implementation and optimization process. The parameters
89 studied include the effects of urease enzyme concentration, degree of temperature, rainwater
90 flushing, oil contamination, and freeze-thaw weathering in winter alpine regions. The impact
91 of these parameters on the performance and effectiveness of MICP technique was related to
92 both the shear strength improvement of bio-treated soil and CaCO_3 precipitation pattern at the
93 micro-scale level. In this study, the introduction of urease enzyme to the soil samples was
94 achieved by the injection of cultivated exogenous pure ureolytic bacteria, which can also be
95 achieved by other methods, such as enrichment of indigenous ureolytic active
96 microorganisms (Burbank et al. 2011) or premixing ureolytic bacteria with soil (Duraisamy
97 and Airey 2015). The aim of the current study is to understand the effect of micro-scale level
98 behavior of MICP (crystal pattern, crystal bonding, bacteria attachment, etc.) under various
99 environmental conditions on the macro-scale mechanical behavior of soil. This is applicable
100 to the MICP process carried out through various introduction methods of urease active
101 bacteria including injection, pre-mixing, and in-situ enrichment. Therefore, the current study
102 is crucial as it provides a deeper understanding of MICP treatment for site conditions, which
103 is crucial before the technique can be applied successfully in the field.

104

105

106

107 **Materials and Methods**

108 ***Soil used***

109 The soil used in the current study was silica sand obtained from Cook Industrial Minerals Pty
110 Ltd, Western Australia. A number of four different particle size distributions, i.e. three
111 poorly-graded and one well-graded, were utilized (Fig. s1). The characteristics of the sand
112 used are listed in Table 1. Sand-1 (uniform sand with 99.6% less than 0.425 mm) was used to
113 investigate the influence of urease enzyme concentration, degree of temperature, rainwater
114 flushing, and oil contamination. Sand-2 (uniform sand with 99.6% less than 0.15 mm), Sand-
115 3 (uniform sand with 99.9% less than 1.18 mm), and Sand-4 (well-graded sand with grain
116 size ranges from 0.053 mm to 2.36 mm) were used to study the impact of freeze-thaw
117 weathering.

118

119 ***Laboratory set-up***

120 The laboratory setup comprised of polyvinyl chloride (PVC) column (45 mm in diameter and
121 180 mm in length) which was cut into half vertically and then glued together using a silicon
122 glue with an inlet (top) connected to a peristaltic pump to allow injection of the reagents into
123 the PVC column and an outlet (bottom) affixed to a U-type tubing. Scour pads and 10 mm
124 thick gravel were placed at the top and bottom of the column, acting as filters to facilitate the
125 spread of the solution during treatment and to prevent the fine sand particles from being
126 flushed out during the treatment cycles. The sand was packed into the column in three
127 consecutive layers, ensuring that each layer was compacted evenly to achieve at least 95% of
128 the maximum dry density (Table 1) so as to maintain consistency of experiments.

129

130 ***Bacterial suspension and cementation solution***

131 The urease active bacteria used in the current experiments were *Bacillus sp.* isolated from a
132 previous work carried out by Al-Thawadi and Cord-Ruwisch (2012). The bacteria were

133 cultivated in a sterile aerobic batch growth medium consisting of 20 g/L yeast extract, 0.17 M
134 ammonia sulphate, and 0.1 mM NiCl₂, with a pH value of 9.25. The cultivated bacteria were
135 collected at the stationary phase of the culture growth after 24 hours of incubation at 28°C.
136 The optical density (OD₆₀₀) of the harvested culture varied between 2–2.5, and the urease
137 activity was approximately 10 U/mL (1 U = 1 μmol urea hydrolyzed per minute). The culture
138 was stored at 4°C refrigerator for no longer than one week prior to use. The cementation
139 solution used in the present study consisted of 1 M anhydrous calcium chloride (110.98 g/L)
140 and 1 M urea (60.06 g/L).

141

142 *MICP treatment process*

143 Except elsewhere stated, the process of MICP treatment was as follows. The PVC column
144 was fully saturated with water at 100% degree of saturation prior to MICP treatment to
145 ensure a relatively controlled flow field during the treatment injections. This was carried out
146 using the upward flow method that facilitates the removal of the air voids from inside of the
147 soil sample. Then, the MICP treatment was employed using the down flow injection method.
148 In order to keep the soil sample fully saturated throughout the treatment, the water level in
149 the external U-type tubing attached to the bottom of the PVC column was maintained equally
150 to the top of the PVC column.

151

152 A two-phase injection scheme was employed for the MICP treatment (except elsewhere
153 stated) by injecting a half void volume of bacteria culture followed by injecting a half void
154 volume of cementation solution (bacterial placement phase), as recommended by Martinez et
155 al. (2013) and Cheng and Cord-Ruwisch (2014). Then the column was cured for 24 hours to
156 allow for bonding of bacteria with the sand particles. Full void volume of cementation
157 solution was then injected into the sand column and was left to cure for 24 hours to allow for
158 calcite precipitation. For each individual sand column, treatment through the cementation

159 solution was repeated several times to gain different degrees of cementation, and the
160 ammonium content and bacterial activity in the effluent of each treatment was monitored.

161

162 *Determination of CaCO₃ content*

163 The calcium carbonate content of treated soil samples was determined by adding solution of 2
164 mL of 2M hydrochloric acid (HCl) to 1–2 g of dry crushed cemented sample, and the volume
165 of CO₂ gas was then measured using a U-tube manometer under standard conditions of 25°C
166 at 1 atm (Whiffin et al. 2007). The actual amount of CaCO₃ was calculated based on an
167 established relationship between the volume of CO₂ gas and amount of pure analytical grade
168 CaCO₃ powder.

169

170 **Soil Properties Investigated**

171 *Permeability*

172 The permeability tests were carried out using the constant head permeability method in
173 accordance with the Australian Standards (2001). The tests were conducted inside the PVC
174 column, where the treated soil samples were still intact, instead of using the standard mold
175 specified in the guidelines. The permeability of soil samples was taken before and after
176 treatment.

177

178 *Unconfined compressive strength (UCS)*

179 After MICP treatment, the treated sand samples were flushed with at least five void volume
180 of tap water to wash away all excess soluble salts prior to UCS experiments. Before the tests
181 were carried out, the sand samples were dried at 105°C for at least 24 hours. The UCS tests
182 were conducted on specimens with selected aspect diameter-to-height ratios of 1:1.5 to 1:2.
183 The axial load was applied at a constant rate of 1.0 mm/min.

184

185 ***Microstructure analysis***

186 To characterize the shapes and location of precipitated CaCO₃ and to investigate the bonding
187 behavior between the grain hosts and bio-cementation agent, microscopy analysis was
188 conducted on the bio-treated soil samples. Before conducting the microscopy investigation,
189 all bio-treated samples were flushed with tap water and dried at 60°C for 24 hours, and were
190 then crashed to small pieces and coated with gold under vacuum conditions. The microscopy
191 investigation was carried out using the available scanning electron microscopy (SEM),
192 PHILIPS XL20 scanning electron microscope (Eindhoven, The Netherlands).

193

194 **Environmental Parameters Investigated**

195 In order to investigate the influence of various environmental conditions on the mechanical
196 and geotechnical response of bio-cemented soils, some key parameters including the urease
197 enzyme concentration (i.e. bacterial cell concentration), degree of temperature, rainwater
198 flushing, oil contamination, and freeze-thaw cycles were examined and procedure of each
199 parameter is explained below.

200

201 ***Urease enzyme concentrations***

202 Hammad et al. (2013) observed that more rapid CaCO₃ crystals were formed under higher
203 urease activity in agar plates. Earlier study carried out by Nemati et al. (2003) indicated that
204 an increase in the urease concentration enhances the extent of CaCO₃ precipitation. However,
205 no study is available in the literature directly linking the effect of different urease enzyme
206 concentrations on the effective crystal bridging formation and the final strength of bio-
207 cemented soils. In the present study, by either diluting the raw bacterial culture (10 U/mL)
208 with deionized (DI) water or concentrating it via centrifuge, a series of bacterial culture with
209 different urease enzyme concentrations (indicated by various levels of urease activity of 5, 10
210 and 50 U/mL) was obtained and utilized for bio-cementation of Sand-1. The treatment

211 process followed the same procedure of that used for the raw bacterial culture, as stated
212 earlier. The urease activity of bacterial culture was determined by measuring the urea
213 hydrolysis rate of the tested bacterial culture. This was made by recording the change in the
214 ammonium concentration of mixture over 30 mins of reaction period, which consisted of 10
215 ml of 3 M urea solution, 2 ml of bacterial culture, and 8 ml of DI water. The ammonium
216 concentration was determined using the Nessler method (Greenburg et al. 1992), and the
217 correlation between the UCS and CaCO_3 content of bio-cemented soils was examined using
218 different urease enzyme concentrations (i.e. urease activities).

219

220 ***Temperature***

221 The subsurface temperature surrounding MICP treated soils was previously investigated by
222 Ng et al. (2012). It was found that the urease activity, which leads to the rate of CaCO_3
223 crystal precipitation, was increased with the increase in temperature from 10°C to 60°C.
224 Nemati et al. (2003) demonstrated that an increase in temperature (from 20°C to 50°C)
225 enhanced both the production rate of CaCO_3 and extent of the cementation solution
226 conversion in a batch system. However, the effectiveness of crystals formed at different
227 degrees of temperature was not investigated. In the current study, three different temperature
228 scenarios were examined for Sand-1. The temperature values were selected to simulate the
229 subsurface soil temperature in cold regions (4°C), tropical regions (25°C), and arid regions
230 (50°C). During the process of MICP treatment, the sand samples used were placed as
231 follows: (1) inside 4°C refrigerator; (2) room temperature of 25°C; and (3) inside 50°C oven,
232 and the UCS and SEM analysis were conducted for the bio-treated samples.

233

234 ***Rainwater flushing***

235 In the current study, tap water (pH ranges from 6.8-7.2) was used to simulate the effect of
236 heavy rain with rainfall intensity of 50 mm/h (National Meteorological Library 2015) on the

237 MICP process. Sand columns made from Sand-1 were subjected to tap water flushing for
238 about 12 hours. The tap water flushing was conducted immediately or 24 hours after the
239 bacterial placement, which was consisted of sequential injections of a half void volume of
240 bacterial culture (45 mL) and a half void volume of cementation solution (45 mL), as stated
241 earlier. All sand columns were then treated with cementation solution (full void volume) for
242 two times. After treatment, the sand samples were extracted from the PVC columns (by
243 gently cutting the silicon glue and opening the PVC column for sand column extraction) for
244 final UCS (if applicable) and CaCO_3 content measurements.

245

246 *Oil contamination*

247 Hydrocarbon contaminants from oil exploration, transportation, production, and processing
248 can change the behavior of soil and may alter the soil engineering properties, resulting in
249 safety issues in civil engineering structures (Nicholson and Tsugawa 1997; Shroff et al. 1998).
250 In the current study, for the first time, the stabilization of oil-contaminated soil using MICP
251 technology was investigated and evaluated through measurements of UCS and CaCO_3
252 content.

253

254 Dried Sand-1 was contaminated with 5% diesel engine oil (w/w), which obtained a maximum
255 dry density of 17.8 kN/m^3 and corresponding optimum moisture content of 7%. The oil-
256 contaminated soil was treated using two procedures, including the two-phase injection
257 method as described above and the premixing method in which bacterial culture was
258 premixed with sand prior to the application of cementation solution. The latter process will be
259 further explained later.

260

261

262

263 *Freeze-thaw cycles*

264 Destruction of porous materials caused by freezing and thawing has been of a great concern
265 to engineers for more than 200 years (Johnson 1952). As suggested by Litvan (1980), soil
266 grain size distribution and permeability affect soil durability against the freeze-thaw (FT)
267 cycles. Therefore, in the present study, sand samples with three different grain size
268 distributions (i.e. Sand-2 to Sand-4, see Fig. 1 and Table 1), and different permeability values
269 (stated in the result section) were examined. Each bio-cemented sand column was cut into
270 half to obtain diameter-to-height aspect ratios of 1:1.5 to 1:2, followed by exposure to 4-FT
271 and 10-FT cycles prior to UCS experiments. Each procedure of FT cycle was subjected to a
272 12h freeze at -14°C followed by a 12h thaw at the room temperature ($25\pm 1^{\circ}\text{C}$). To ensure
273 that full saturation was achieved, all treated samples were completely immersed in water
274 throughout the FT cycles. The effect of FT cycles on the bio-cemented samples was
275 evaluated by comparing the UCS values before and after the FT cycles.

276

277 **Results and Discussion**

278 *Effect of urease enzyme concentrations*

279 The influence of different urease concentrations on UCS of bio-cemented soil samples was
280 examined by plotting the measured UCS values against CaCO_3 contents (Fig. 1a). It can be
281 seen that for all urease activities, the UCS increases exponentially with the increase of the
282 CaCO_3 content, which is in line with previous results reported by van Paassen et al. (2010b)
283 and Cheng et al. (2013). It can also be seen that for the same amount of CaCO_3 precipitation,
284 the UCS of bio-cemented soil treated with higher urease activity is less than that of the
285 samples treated with lower activity. For instance, at an amount of 0.04 g/g CaCO_3
286 precipitation, the sand sample treated with 50 U/ml urease activity achieved UCS value of
287 around 250 kPa, whereas the sand samples treated with 10 and 5 U/ml urease activity
288 achieved higher UCS values of around 500 and 850 kPa, respectively. This suggests that the

289 CaCO_3 formed slowly, which is due to the slower hydrolysis of urea caused by the lower
290 urease activity, are more effective to form “bridges” that bond the sand grains together in a
291 more effective way. It should be noted that the efficiency in UCS improvement was only
292 slightly improved using the 2 U/ml activity compared to the 5 U/ml (data not shown), and the
293 use of such low urease activity required a significant extension of treatment period to allow
294 for completion of the MICP reaction.

295

296 In Fig. 1b, the measured permeability values of soil samples after MICP treatment were
297 normalized with the initial permeability values and plotted against the CaCO_3 content. As can
298 be seen, all samples show a reduction in permeability with the increase in the amount of
299 CaCO_3 precipitation. Fig. 1b also indicates that the reduction in permeability of bio-cemented
300 samples was mainly controlled by the amount of CaCO_3 precipitation, whereas the level of
301 urease activity used in treatment has a minor impact.

302

303 The micro-feature of precipitated crystals within the sand matrix was examined using SEM
304 (Fig. 2). It can be seen in Fig. 2(a-c) that the CaCO_3 produced at high urease activity formed
305 small crystals of a typical crystal size of 2-5 μm . The agglomerated small crystal precipitates
306 formed thin coating layers (CaCO_3 envelope) with a thickness of around 5 μm covering the
307 individual sand grain surface and bridging the adjacent sand grains. This type of crystal
308 precipitation might not be strong enough to bear high shear strength, which is probably due to
309 the thin and weak “bridging layer” and remaining large gaps between the sand grains. In
310 contrast, the crystals produced at low urease activity were agglomerated and formed large
311 clusters of size of around 20-50 μm [Fig. 2(d-f)]. One important feature in this regard is that
312 although large crystal clusters precipitated on the sand grain surface, the gaps between the
313 sand grains were almost completely filled with crystals (Fig. 2d). It should be noted that the
314 samples presented in Fig. 2 demonstrate similar UCS values but have different CaCO_3

315 contents, suggesting that the crystals pattern formed at lower urease activity is more effective
316 in gaining strength.

317

318 It has been reported in the literature that there are two mechanisms for crystal precipitation in
319 MICP (Stocks-Fischer et al. 1999; DeJong et al. 2006). The first mechanism is that bacterial
320 cells act as nucleation sites for CaCO_3 precipitation. The second mechanism is that the urea
321 hydrolysis produces CO_3^{2-} ions and raises the pH around the cells, favoring the precipitation
322 of CaCO_3 by lowering the solubility. In the current study, it is apparent that development of
323 CaCO_3 is vastly different under different urease activities, in terms of location, size, and
324 shape of crystals. Because the same cementation solution was applied to all samples, it was
325 expected that the bacterial urease activity would be the only factor that can have an impact on
326 the precipitation patterns.

327

328 An explanation of the noted difference in the precipitation patterns may be attributed to the
329 competition between the crystal growth and crystal nucleation. Gandhi et al. (1995) reported
330 that the nucleation of new crystals would compete with the process of crystal growth if
331 nucleation of new crystals prevails over the growth of those exist. In case of high urease
332 enzyme concentration, a high number of bacterial cells were introduced to the soil samples,
333 which were accumulated at the pore “throat” (contact points) and also attached to the sand
334 grain surface. With the presence of abundant bacterial cells acting as nucleation site, the
335 produced carbonate ions may be consumed mainly by nucleation of new CaCO_3 crystals
336 rather than growth of existing crystals, resulting in an abundance of small crystals. These
337 numerous small crystals would develop to form dense crystal layers with continuous supply
338 of cementation solution. In contrast, in case of low urease enzyme concentration (i.e. low
339 urease activity/bacteria concentration), the nucleation site was limited by the small number of
340 bacterial cells. Otterstedt and Brandreth (2013) stated that the final crystal size is inversely

341 related to the number of nuclei. For low urease activity, the presence of high concentration of
342 calcium (i.e. 1 M in the current study) and increased super-saturation in the solution due to
343 urea hydrolysis would result in accumulating of precipitation over the initial small crystals,
344 leading to formation of larger crystal sizes rather than new small crystals. It is worthwhile
345 noting that using different ureolytic bacteria, with either higher or lower specific urease
346 activity (urase activity per cell) compared to the current strain, might lead to different results
347 to those presented herein. This is because in order to obtain the same urease activity as
348 obtained in the current study, different amount of biomass might be required, leading to
349 different number of nucleation site and hence, affecting the patterns of precipitated crystals
350 potentially.

351

352 The findings obtained from this study indicate that the efficacy (strength per mass of calcite)
353 of larger calcite crystals precipitated at the gaps between the sand grains is higher than that
354 obtained from smaller crystals randomly precipitated throughout the sand matrix. This is
355 consistent with the described phenomena in the literature. For example, Cheng et al. (2013)
356 found that bridging crystals were formed by restricting the pore water at the contact points
357 between the sand grains, showing more efficiency in terms of strength improvement
358 compared to crystals randomly precipitated. Al Qabany and Soga (2013) demonstrated that
359 using cementation solution of low concentration may yield to higher sample strengths, which
360 may be attributed to the larger amount of precipitation at the particle contacts, similar to the
361 findings of Okwadha and Li (2010) and Cheng et al. (2014). In particular, the significance of
362 calcium carbonate precipitation pattern on properties of MICP treated soils was highlighted
363 by many researchers (e.g., Al Qabany and Soga 2013; Okwadha and Li 2010; Cheng et al.
364 2013). Martinez and DeJong (2009) reported that the degradation of bio-cemented sand
365 particles at the micro scale level was governed by the calcite bonds between the silica sand
366 grains. Accordingly, it was expected that the shear strength of sand may not be directly

367 proportional to the amount of calcite content. Those crystals filling the gaps between the sand
368 grains and forming effective bridges contribute to the pathway of load transferred between
369 the soil particles; thus, improve the soil stiffness and strength.

370

371

372 *Effect of degree of temperature*

373 The effect of various degrees of temperature equal to 4, 25 and 50°C on strength
374 improvement of bio-cemented soil was examined and presented in Fig. 3. It can be seen that
375 all UCS values of bio-treated sand samples were exponentially increased with the increase in
376 CaCO₃ content, irrespective of the applied temperature. However, the strength improvement
377 as per the amount of crystals produced was higher at 25°C compared to that at temperature of
378 either extremely low (4°C) or high (50°C). The crystals formed at the highest temperature of
379 50°C was the least efficient to gain strength improvement.

380

381 The crystals microstructure analysis indicates that MICP treatment at 50°C results in crystal
382 distribution over the entire sand grain surface, with a typical individual crystal size of 2-5 μm
383 [Fig. 4(e-f)]. For such samples, the individual CaCO₃ crystals possessed similar size and were
384 well-distributed spatially and also covered the surface of the sand grains as a coating-like
385 layer. However, the sand grains were not effectively connected because of the remaining
386 large gaps [Fig. 4(e-f)]. For samples treated at the ambient temperature, it was found that the
387 average crystal size increased by 10 times (individual crystals size between 20 to 50 μm)
388 compared to that formed at 50°C. These large crystals were found to precipitate on the grain
389 surface, covering the contact areas of the sand grains [Fig. 4(c-d)]. This type of crystals
390 distribution pattern was also found in the samples treated at 4°C, and small crystal size was
391 observed [Fig. 4(a-b)].

392

393 The kinetics of crystallization indicates that activated energy, which is a function of
394 temperature and relative supersaturation degree, has a strong impact on the rate of nucleation
395 and crystal growth. It is the relationship between the competing kinetic rates of nucleation
396 (birth of new crystal nuclei) and crystal growth (increase in size of crystals) that determines
397 the size distribution of crystals. The higher the temperature the lower the activation energy
398 barrier as well as the faster the rate of nucleation of CaCO₃ precipitation (Wojtowicz 1998).
399 The faster nucleation rate may induce excess nucleation sites, which would cause smaller
400 average crystal size as it was found in the samples treated at 50°C. It is worthwhile noting
401 that although the nucleation rate was low at low temperature of 4°C, small size of crystals
402 was also observed. This is possibly due to the slow crystal growth at low temperature due to
403 the low relative supersaturation degree as a result of the low urease activity at low
404 temperature (Sahrawat 1984). A decrease in the relative supersaturation led to a decrease in
405 both the crystal nucleation rate and growth rate. As stated earlier, the final crystal size
406 distribution is dependent on the competition between these two rates.

407

408 The precipitation of CaCO₃ in MICP is a very complex process because of the involvement
409 of bacteria acting as nucleation site and CO₃²⁻ ion producer. Therefore, if different amount of
410 bacteria is applied, the precipitation pattern can be different from what was presented in the
411 current study. It is evident from Fig. 2(a-c) that large amount of bacteria (high activity 50
412 U/ml) at the ambient temperature would result in abundant nucleation sites (numerous
413 bacterial cells) and high relative supersaturation degree (high urease activity). As a result, the
414 precipitation pattern obtained under this environmental condition could be similar to that
415 obtained at 50°C with low amount of bacteria (10 U/ml) [Fig. 4(e-f)]. Generally, temperature
416 can affect many physical, chemical, and biological properties of MICP system. For example,
417 temperature can affect the urease activity, which in turn influences the urea hydrolysis rate,
418 CO₃²⁻ production rate, and consequent crystal growth rate. The solubility of CaCO₃ crystals

419 also varies with temperature. Therefore, further investigation on this complex process is
420 worthwhile to carry out in future development of the current study. Overall, based on the
421 results obtained from the current study of different urease concentrations and temperatures, it
422 can be concluded that large size crystals located at the gaps between the sand grains are
423 deemed to be effective crystals, which contribute the most to the strength gain of bio-
424 cemented soils.

425

426 *Effect of rainwater flushing*

427 In the current study, tap water flushing was made to determine the impact of intensive rainfall
428 towards CaCO_3 precipitation and corresponding soil stabilization. The control sample (i.e. no
429 water flushing) was fully cemented (Fig. 5a). In contrast, the samples encountered with water
430 flushing during the treatment process were partly cemented or completely non-cemented [Fig.
431 5(b-c)]. For the control sample, the chemical conversion efficiency, which is defined as the
432 percentage of injected urea and calcium chloride that precipitate as CaCO_3 , was found to
433 reduce from about 95% to 50% throughout the MICP process (Fig. 6a). The decrease in
434 chemical conversion efficiency was probably explained by the loss of urease activity due to
435 the encapsulation of the bacterial cells by precipitated crystals. The water flushing caused
436 significant decrease in the chemical conversion efficiency down to less than 5%, irrespective
437 of the waiting period applied to the bacterial attachment. The negative impact of water
438 flushing on bio-cementation was also demonstrated by the low degree of cementation and
439 final CaCO_3 content measurements. Less than 0.3% (0.003 g/g sand) of crystals content was
440 detected in the samples subjected to water flushing, whereas 10 times more (0.043 g/g sand)
441 crystals were found in the control sample with a detectable UCS of about 260 kPa (Fig. 6b).

442

443 The low chemical conversion efficiency and CaCO_3 precipitation after water flushing may be
444 due to the washout of bacteria and substrate. For successful bio-cementation, it is necessary

445 that the bacteria are introduced into the soil first and immobilized, then followed by
446 application of cementation solution that contains urea and calcium chloride. Many authors
447 have shown that the adsorption of bacteria increases with increasing the salinity of bacterial
448 suspension (Scholl et al. 1990; Torkzaban et al. 2008). By flushing low salinity solutions
449 after the bacterial suspension, a large part of the adsorbed bacteria can be remobilized from
450 the solid surface into the liquid phase (Harkes et al. 2010). This suggests that in real
451 application the rainwater flushing during MICP bio-cementation can impact the effectiveness
452 of MICP treatment by washing out the immobilized bacterial cells and reducing the chemical
453 conversion efficiency. In order to overcome this problem, a new way of bacterial fixation,
454 which can prevent bacterial cells from being washed out by the low salinity solution (i.e.
455 rainwater) will be investigated in future work.

456

457 *Effect of oil contamination*

458 Oil contamination can alter the soil engineering properties, resulting in safety issues in
459 relation to civil engineering infrastructures. Also, oil-contaminated soil represents the worst
460 case scenario of hydrophobic soil particle surface property, which might have a negative
461 impact on bacteria immobilization. As expected, the initial trial of stabilization of oil
462 contaminated soils using MICP via the normal two-phase injection method did not succeed
463 (data not shown). This suggests that the traditional bacterial immobilization method does not
464 work effectively for oil-contaminated soils due to the hydrophobic surface of oil-
465 contaminated soil particles, resulting in poor bacterial attachment. In fact, the impact of
466 hydrophobic oil on bacteria attachment is a function of the bacterial culture properties. The
467 bacterial cells (i.e. oil-degrading strain), which are hydrophobic can attach to the hydrophobic
468 surfaces (Rosenberg 2006); however, bacteria with hydrophilic characteristics prefer
469 hydrophilic surface (An and Friedman 1998). In order to improve the bacterial retention,
470 premixing of bacteria with soil in the presence of 100 mM CaCl₂ was applied. The presence

471 of CaCl_2 acted as flocculent and induced cells coagulation. This coagulation of bacterial cells
472 was found not to significantly lower the urease activity, as reported by Al-Thawadi (2008).
473 To provide a sufficient urease activity, 180 mL of bacterial culture containing 100 mM CaCl_2
474 was used and concentrated into 25 mL volume using centrifuge. The concentrated bacterial
475 flocs were then mixed with the oil-contaminated soil to reach the optimum moisture content.
476 The mixture of bacterial flocs and soil was compacted thoroughly in the PVC column to gain
477 the maximum dry density, which was then repeatedly treated 5 times by the cementation
478 solution.

479

480 The UCS results indicated that by increasing the CaCO_3 content from 0.035 to 0.054 g/g
481 sand, strength of oil contaminated soil was improved significantly from about 150 kPa to 400
482 kPa (see Fig. s2). Accordingly, soil stiffness was also improved from 10.7 MPa to 68.3 MPa.
483 The failure mechanisms of bio-treated oil contaminated soil were consistent with previous
484 observations on cemented pure silica sand (Cheng et al. 2013). For the weak sample of UCS
485 = 150 kPa, the broken cores completely lost strength at the grain scale around the failure
486 plane. On the other hand, the strong sample of UCS = 400 kPa, longitudinal tensile cracks
487 along the sample were clearly observed.

488

489 *Effect of freeze-thaw cycles*

490 Litvan (1980) found that porous solids with high porosity or permeability usually have a good
491 service record after FT action. Cheng et al. (2013) found that microbially induced CaCO_3
492 crystals covered the connecting points between the sand grains and thus provided key
493 bonding force within the soil matrix against the FT cycles. This bonding behavior might be
494 different for different PSD sand samples. Therefore, before carrying out the FT cycles, it was
495 necessary to investigate the mechanical behavior of different PSD sand samples after MICP
496 treatment.

497 Fig. 7 shows that the UCS increases exponentially with the increase in the CaCO_3 content. At
498 low level of CaCO_3 content (below 0.04 g/g sand), similar UCS improvement was obtained
499 for all different PSD samples; however, the improvement varied at high level of crystal
500 content (above 0.05 g/g sand). At high CaCO_3 content, Sand-3 showed the least effective
501 strength improvement because it required the highest amount of crystals to gain strength
502 similar to that of the other PSD samples. For the two types of uniform sand tested herein, the
503 crystals were more effective in improving the strength of soil of smaller grain size, which is
504 consistent with previous findings obtained by Ismail et al. (2002b). This is probably due to
505 the increase in number of contact points, which provide better location for crystals to
506 precipitate, and the decrease in stress acting per particle contact. For Sand-4 (well-graded),
507 the effectiveness of crystal precipitation in terms of strength improvement was greater than
508 that of the uniform coarse sand (i.e. Sand-3) but less than the uniform fine sand (i.e. Sand-2).
509 According to Schiffman and Wilson (1958), the greater the percentage of the coarser fraction,
510 the smaller the available grain surfaces for grout adhesion and the lower the internal tension
511 in the grouted mass. Although the used well-graded sand has the highest density compared to
512 the fine sand, it possesses less contact points and grain surface due to its large percentage of
513 coarse particles. Therefore, the crystals formed for well-graded sand were less effective
514 compared to those formed for fine sand.

515

516 The effect of FT cycles on the mechanical performance of different PSD sand samples treated
517 with MICP is illustrated in Fig. 8. Generally speaking, it can be observed that an increase in
518 the number of FT cycles is associated with a decrease in the compressive strength, for all
519 uniform sand specimens (Fig. 8 (a-b)). The main reason for the strength decrease after FT
520 cycles is due to the formation and growth of micro-cracks generated due to the tensile
521 stresses around the soil particles when the pore water turns into ice during the freezing
522 process. In theory, higher porosity and permeability allow more rapid water mass transfer in

523 the sand matrix, which can increase the FT resistance. However, in the current study, the fine
524 uniform sand (0.15 mm in size) of less porosity and smaller pore size was more durable
525 against the FT cycles compared to the coarse sand (1.18 mm in size) of higher porosity and
526 larger pore size. Smith et al. (1929) found that the average number of contacts per sphere
527 increases with the decrease in porosity. Therefore, for finer sand, the larger number of inter-
528 particle contact points favored more bridging crystals formed at the contact points, which
529 reduced the acting tensile stress per particle contact; hence, resulted in higher durability. Fig.
530 8c shows that the FT cycles have a minor impact on the well-graded sand. The main reason
531 for the high durability of MICP well-graded sand is probably due to the unique characteristics
532 of having high number of inter-particle contact points (attributed to the presence of fine sand)
533 and high permeability, as well as large pore size (attributed to the presence of coarse sand).
534 Overall, it can be concluded that the influence of FT cycles on soil strength and durability
535 depends on the soil porosity, pore size, and bonding behavior of MICP in the soil matrix.

536

537 *Implication for civil engineering applications*

538 In civil engineering applications such as soil stabilization for transportation subgrades and
539 embankments, adequate MICP strength improvement can be achieved by forming sufficient
540 CaCO_3 bonds between the soil grains. The ability to produce CaCO_3 crystals with high
541 efficacy is thus highly desirable for cost minimization. The findings obtained from the current
542 study show that different urease activities can result in different micro-scale crystal
543 precipitation patterns, leading to varied efficacy in obtaining the macro-scale strength values.
544 This potentially has implications in terms of how MICP treatment can be applied more
545 economically in engineering practice. Low level of urease activity associated with an
546 optimum operating temperature could result in larger calcium carbonate crystals precipitated
547 in the voids of soil grains, which can lead to a more effective strength improvement with less
548 consumed chemicals.

549 In other civil engineering applications such as control of seepage-induced internal erosion of
550 dams, it is important to immobilize the urease active bacteria and urease activity within the
551 target zones so that sufficient CaCO_3 can be produced throughout the entire treated soil. The
552 experimental observations shown in this paper indicated poor immobilization through the
553 two-phase injection method after tap water flushing, which implies that the current bacteria
554 fixation method might not be applicable to field application of MICP during rainy days. It is
555 thus considered essential to develop a new bacteria fixation method, which can further extend
556 MICP application to continuous water flow regions.

557

558 Soils at high latitude or elevation usually freeze during winter. Under this environmental
559 condition, geotechnical engineering foundations that are exposed to FT cycles can be subject
560 to significant structure damages. In such a case, FT cycles induce uneven stresses within the
561 soil, resulting in a decrease in soil stability. Given the improvement in UCS values of the
562 sand tested in the current study, it can be confirmed that MICP can be used as a viable
563 solution to improve the properties of uncemented soils by creating cemented soil bodies that
564 have high durability against FT cycles. The high durability of MICP treated soils against FT
565 cycles is attributed to the sufficient contact points in the soil matrix and large pore size and
566 permeability of soil. This characteristic enhances the efficacy of MICP cementing agents in
567 bridging the particle-to-particle contacts, and in the meanwhile allows a rapid water mass
568 transfer in the sand matrix.

569

570 **Conclusions**

571 This paper presented a series of experimental results in relation to the mechanical behavior of
572 silica sand stabilized using microbially induced calcite precipitation (MICP) under different
573 environmental conditions. The formation of large agglomerated crystal clusters filling the
574 gaps between the sand grains showed high efficiency in improving the compressive strength

575 of bio-treated soils. Such optimum crystal precipitation pattern was found to be obtained at
576 low urease concentration and ambient temperature of 25°C. Trials of “rain” flushing and oil
577 contaminated soil stabilization have clearly shown the bacterial attachment using the two-
578 phase injection method can be deteriorated by flushing of low ionic strength water (i.e. tap
579 water, rain water) or hydrophobic surface of sand grain particles (i.e. oil-contaminated soils).
580 Alternatively, premixing of bio-flocs with oil-contaminated soil was able to achieve sufficient
581 retention of bacteria and urease activity, leading to successful soil stabilization of significant
582 UCS improvement. The FT cycle tests have shown that the durability of bio-cemented soils
583 was varied depending on the particle size distribution. The soil matrix of well-graded sand
584 allowed sufficient amount of contact points for effective crystals that create strong bonding,
585 large pore size, and high permeability, leading to a rapid water mass transfer in the sand
586 matrix and contributing to the resistance of the FT cycles.

587

588 **Acknowledgement**

589 The authors acknowledge the assistance provided by Lorenzo Lorio and Danial Zubair
590 (graduate engineers from Curtin University, Australia) in carrying out some experiments of
591 this work.

592

593 **Supplemental Data**

594 Figs. s1-s2 are available online in the ASCE library (ascelibrary.org)

595

596 **References**

597 Al Qabany, A., Soga, K., and Santamarina, C. (2012). “Factors affecting efficiency of
598 microbially induced calcite precipitation.” *J. Geotech. Geoenviron. Eng.*,
599 10.1061/(ASCE)GT.1943-5606.0000666, 992–1001.

600 Al Qabany, A., and Soga, K. (2013). "Effect of chemical treatment used in MICP on
601 engineering properties of cemented soils." *Géotechnique*, 63(4), 331–339.

602 Al-Thawadi, S. M. (2008). "High strength in-situ biocementation of soil by calcite
603 precipitating locally isolated ureolytic bacteria." Ph.D. thesis, Murdoch Univ., Perth,
604 Australia.

605 Al-Thawadi, S. M., and Cord-Ruwisch, R. (2012). "Calcium carbonate crystals formation by
606 ureolytic bacteria isolated from Australian soil and sludge." *J. Adv. Sci. Eng. Science Res.*,
607 2(1), 13–26.

608 An, Y. H., and Friedman, J. R. (1998). "Concise review of mechanisms of bacterial adhesion
609 to biomaterial surface." *J. Biomed. Mater. Res.*, 43(3), 338-348.

610 Australian Standards. (2001). "Methods of testing soils for engineering purposes - Soil
611 strength and consolidation tests - Determination of permeability of a soil - Constant head
612 method for a remoulded specimen." Australia.

613 Burbank, M. B., Weaver, T. J., Green, T. L., Williams, B. C., and Crawford, R. L. (2011).
614 "Precipitation of calcite by indigenous microorganisms to strengthen liquefiable soils."
615 *Geomicrobiol. J.*, 28(4), 301-312.

616 Cheng, L., Cord-Ruwisch, R., and Shahin, M. A. (2013). "Cementation of sand soil by
617 microbially induced calcite precipitation at various degrees of saturation." *Can. Geotech.*
618 *J.*, 50(1), 81–90.

619 Cheng, L., and Cord-Ruwisch, R. (2014). "Upscaling effects of soil improvement by
620 microbially induced calcite precipitation by surface percolation." *Geomicrobiol. J.*, 31(5),
621 396–406.

622 Cheng, L., Shahin, M. A., Cord-Ruwisch, R. (2014). "Bio-cementation of sandy soil using
623 microbially induced carbonate precipitation for marine environments." *Géotechnique*,
624 64(12), 1010–1013.

625 Chou, C. W., Seagren, E. A., Aydilek, A. H., and Lai, M. (2011). “Biocalcification of sand
626 through ureolysis.” *J. Geotech. Geoenviron. Eng.*, 10.1061/(ASCE)GT.1943-
627 5606.0000532, 1179–1189.

628 DeJong, J. T., Fritzges, M. B., and Nüsslein, K. (2006). “Microbially induced cementation to
629 control sand response to undrained shear.” *J. Geotech. Geoenviron. Eng.*,
630 10.1061/(ASCE)1090-0241(2006)132:11(1381), 1381–1392.

631 DeJong, J. T., Mortensen, B. M., Martinez, B. C., and Nelson, D. C. (2010). “Bio-mediated
632 soil improvement.” *Ecol. Eng.*, 36(2), 197–210.

633 DeJong, J. T., Martinez, B. C., Ginn, T. R., Hunt, C., Major, D., and Tanyu, B. (2014).
634 “Development of a scaled repeated five-spot treatment model for examining microbial
635 induced calcite precipitation feasibility in field applications.” *Geotech. Test. J.*, 37(3),
636 424–435.

637 Duraisamy, Y., and Airey, D. W. (2015). “Performance of biocemented Sydney sand using ex
638 situ mixing technique.” *J. Deep. Found. Inst.*, 9(1), 48-56.

639 Feng, K., and Montoya, B. M. (2015). “Influence of confinement and cementation Level on
640 the behavior of microbial-induced calcite precipitated sands under monotonic drained
641 loading.” *J. Geotech. Geoenviron. Eng.*, 10.1061/(ASCE)GT.1943-5606.0001379,
642 04015057.

643 Fujita, Y., Ferris, F. G., Lawson, R. D., Colwell, F. S., and Smith, R. W. (2000). “Subscribed
644 content calcium carbonate precipitation by ureolytic subsurface bacteria.” *Geomicrobiol.*
645 *J.*, 17(4), 305–318.

646 Gandhi, K. S., Kumar, R., and Doraiswami, R. (1995). “Some basic aspects of reaction
647 engineering of precipitation processes.” *Ind. Eng. Chem. Res.*, 34(10), 3223–3230.

648 Greenburg, A.E., Clesceri, L.S., and Eaton, A.D. (1992). *Standard Methods for the*
649 *Examination of Water and Wastewater*, 18th ed. American Public Health Association,
650 Washington.

651 Hammad, I. A., Talkhan, F. N., and Zoheir, A. E. (2013). "Urease activity and induction of
652 calcium carbonate precipitation by *Sporosarcina pasteurii* NCIMB 8841." *J. App. Sci.*
653 *Res.*, 9(3), 1525–1533.

654 Harkes, M. P., van Paassen, L. A., Booster, J. L., Whiffin, V. S., and van Loosdrecht, M. C.
655 M. (2010). "Fixation and distribution of bacterial activity in sand to induce carbonate
656 precipitation for ground reinforcement." *Ecol. Eng.*, 36(2), 112–117.

657 Ismail, M. A., Joer, H. A., Sim, W. H., and Randolph, M. F. (2002a). "Effect of cement type
658 on shear behavior of cemented calcareous soil." *J. Geotech. Geoenviron. Eng.*,
659 10.1061/(ASCE)1090-0241(2002)128:6(520), 520–529.

660 Ismail, M.A., Joer, H.A., Randolph, M.F., and Meritt, A. (2002b). "Cementation of porous
661 materials using calcite." *Géotechnique*, 52(5), 313–324.

662 Johnson, A. W. (1952). "Frost action in roads and airfield-a review of the literature." *Special*
663 *Report No. 1*, Highway Research Board, Washington, USA.

664 Lin, H., Suleiman, M. T., Brown, D. G., Kavazanjian, E. (2015). "Mechanical behavior of
665 sands treated by microbially induced carbonate precipitation." *J. Geotech. Geoenviron.*
666 *Eng.*, 10.1061/(ASCE)GT.1943-5606.0001383.

667 Litvan, G. G. (1980). "Freeze-thaw durability of porous building materials." *Proc., 1st*
668 *international conference of durability of building materials and components*, P. J. Sereda,
669 and G. G. Litvan, ed., Ottawa, Canada, 455-463.

670 Martinez, B. C., and DeJong, J. T. (2009). "Bio-mediated soil improvement: Load transfer
671 mechanisms at micro- and macro- scales." *Proc. of the 2009 U.S.-China Workshop on*
672 *Ground Improvement Technologies*, ASCE, Reston, VA, 242–251.

673 Martinez, B., J. DeJong, T. Ginn, B. Montoya, T. Barkouki, C. Hunt, B. Tanyu, and D.
674 Major. (2013). "Experimental optimization of microbial-induced carbonate precipitation
675 for soil improvement." *J. Geotech. Geoenviron. Eng.*, 10.1061/(ASCE)GT.1943-
676 5606.0000787, 587–598.

677 Montoya, B. M., and DeJong, J. T. (2015). “Stress-strain behavior of sands cemented by
678 microbially induced calcite precipitation.” *J. Geotech. Geoenviron. Eng.*,
679 10.1061/(ASCE)GT.1943-5606.

680 Mortensen, B. M., Haber, M., DeJong, J. T., Caslake, L. F., and Nelson, D. C. (2011).
681 “Effects of environmental factors on microbial induced calcite precipitation.” *J. Appl.*
682 *Microbiol.*, 111(2), 338–349.

683 National Meteorological Library (2015). “Water in the atmosphere.”
684 <http://www.metoffice.gov.uk/media/pdf/4/1/No._03_-_Water_in_the_Atmosphere.pdf>
685 (Jul. 22, 2015).

686 Nemati, M., and Voordouw, G. (2003). “Modification of porous media permeability, using
687 calcium carbonate produced enzymatically in situ.” *Enzyme Microb. Technol.*, 33(5), 635–
688 642.

689 Nicholson, P. G., and Tsugawa, P. R. (1997). “Stabilization of diesel contaminated soil with
690 lime and fly ash admixtures.” *Fuel Energy Absrt.*, 38(4), 269–269.

691 Ng, W. S., Lee, M. L., and Hii, S. L. (2012). “An overview of the factors affecting microbial-
692 induced calcite precipitation and its potential application in soil improvement.” *World*
693 *Acad. Sci. Eng. Technol.*, 6(2), 683–689.

694 Okwadha, G. D., and Li, J. (2010). “Optimum conditions for microbial carbonate
695 precipitation.” *Chemosphere*, 81(9), 1143–1148.

696 Otterstedt, J. E., and Brandreth, D. A. (2013). *Small Particles Technology*, Springer, USA.

697 Rosenberg, M. (2006). “Microbial adhesion to hydrocarbons: twenty-five years of doing
698 MATH.” *FEMS Microbial. Lett.*, 262, 129-134.

699 Sahrawat, K. (1984). “Effects of temperature and moisture on urease activity in semi-arid
700 tropical soils.” *Plant Soil*, 78(3), 401–408.

701 Schiffman, R., and Wilson, C. (1958). “The mechanical behaviour of chemically treated
702 granular materials.” *Proc. Am. Soc. for Test. Mater.*, 58, 1218–1244.

703 Scholl, M. A., Mills, A. L., Herman, J. S., and Hornberger, G. M. (1990). "The influence of
704 mineralogy and solution chemistry on the attachment of bacteria to representative aquifer
705 materials." *J. Contam. Hydrol.*, 6, 321–336.

706 Shroff, A. V., Shah, D. L. and Shah, S. J. (1998). "Characteristics of fuel oil contaminated
707 soil and remedial measures—A case study." *Proc. of Indian Geotech. Conf.*, India, 49–51.

708 Smith, W. O., Foote, P. D., and Busang, P. F. (1929). "Packing of homogeneous spheres."
709 *Phys. Rev.*, 34(9), 1271-1274.

710 Stocks-Fischer, S., Galinat, J. K., and Bang, S. S. (1999). "Microbiological precipitation of
711 CaCO₃." *Soil Biol. Biochem.*, 31(11), 1563–1571.

712 Torkzaban, S., Tazehkand, S. S., Walker, S. L., and Bradford, S. A. (2008). "Transport and
713 fate of bacteria in porous media: coupled effects of chemical conditions and pore space
714 geometry." *Water Resour. Res.*, 44, 1–12.

715 van Paassen, L. A., Daza, C. M., Staal, M., Sorokin, D. Y., Van der Zon, W., and Van
716 Loosdrecht, M. C. M. (2010a). "Potential soil reinforcement by microbial denitrification."
717 *Ecol. Eng.*, 36(2), 168–175.

718 van Paassen, L.A., Ghose, R., van der Linden, T.J.M., van der Star, W.R.L., and van
719 Loosdrecht, M.C.M. (2010b)." Quantifying biomediated ground improvement by
720 ureolysis: large-scale biogROUT experiment." *J. Geotech. Geoenviron. Eng.*,
721 10.1061/(ASCE)GT.1943-5606.0000382, 1721–1728.

722 Whiffin, V. S., van Paassen, L. A., and Harkes, M. P. (2007). "Microbial carbonate
723 precipitation as a soil improvement technique." *Geomicrobiol. J.*, 24(5), 417–423.

724 Wojtowicz, J. A. (1998). "Factors affecting precipitation of calcium carbonate." *J. Swimming
725 Pool Spa Ind.*, 3(1), 18-23.

726

727

728 Captions:

729 **Fig. 1.** Effect of the different urease activity on (a) UCS and (b) permeability of the bio-
730 cemented samples

731 **Fig. 2.** SEM images of bio-cemented samples treated with different urease activities (a-c: 50
732 U/mL, UCS = 713 kPa, and CaCO₃ content = 0.061 g/g sand; d-f: 5 U/mL, UCS=709 kPa,
733 and CaCO₃ content = 0.039 g/g sand)

734 **Fig. 3.** Effect of the temperature on the UCS of the bio-cemented samples

735 **Fig. 4.** SEM images of bio-cemented samples treated at different temperatures (a-b: 4°C,
736 UCS = 108 kPa and CaCO₃ content = 0.021 g/g sand; c-d: 25°C, UCS=245 kPa and CaCO₃
737 content = 0.028 g/g sand; e-f: 50°C, UCS=121 kPa and CaCO₃ content = 0.034 g/g sand)

738 **Fig. 5.** Images of MICP treated samples (removed from the PCV columns prior to UCS test)
739 subjected to water flushing during the treatment process: (a) control with no water flushing;
740 (b) water flushing after 24 hours of bacterial placement; and (c) water flushing immediately
741 after bacterial placement

742 **Fig. 6.** MICP treated samples subject to water flushing during the treatment process: (a)
743 chemical conversion efficiency; and (b) UCS and CaCO₃ content

744 **Fig. 7.** UCS of different PSD sand samples treated with different amount of MICP

745 **Fig. 8.** Effect of FT cycles on UCS of different PSD sands treated with different amount of
746 MICP: (a) 0.15 mm uniform sand; (b) 1.18 mm uniform sand; and (c) well-graded sand

747

748

749

750

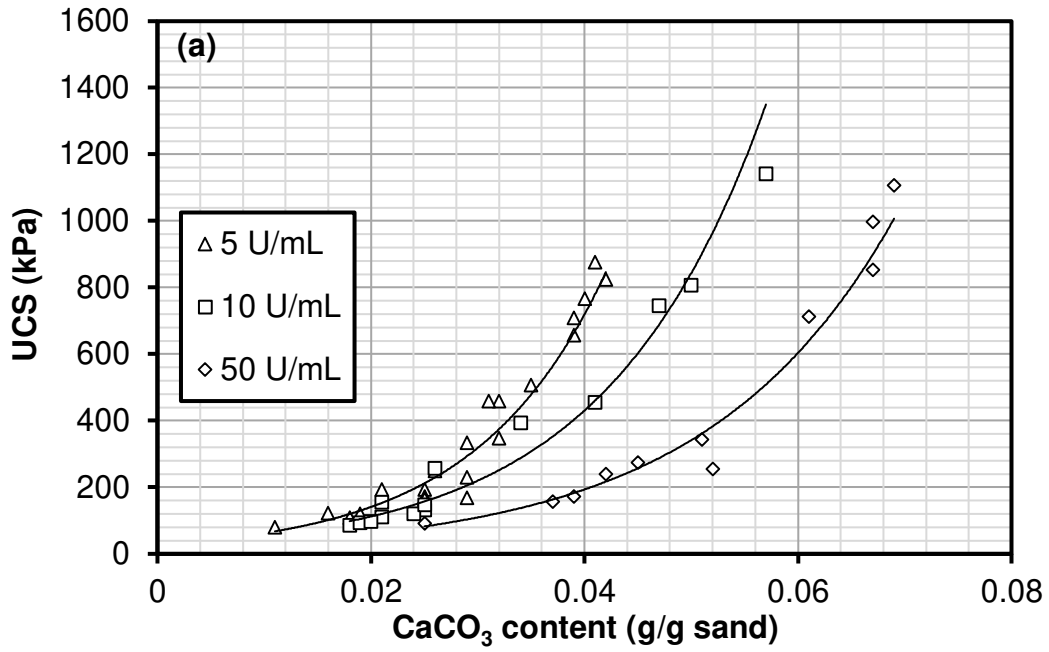
751

752

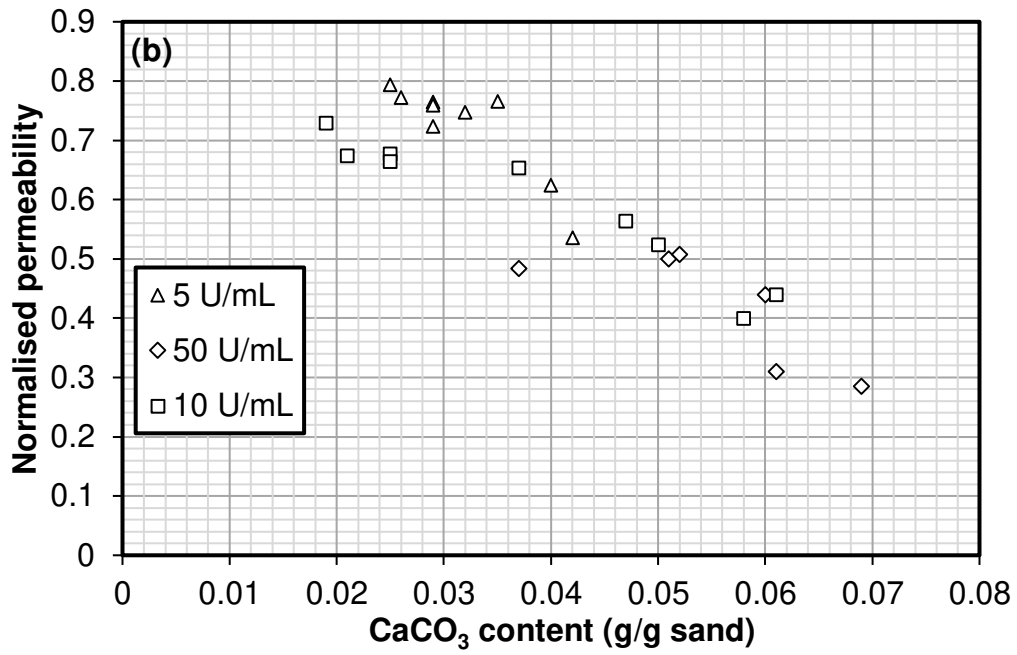
753

754

755 Fig. 1.



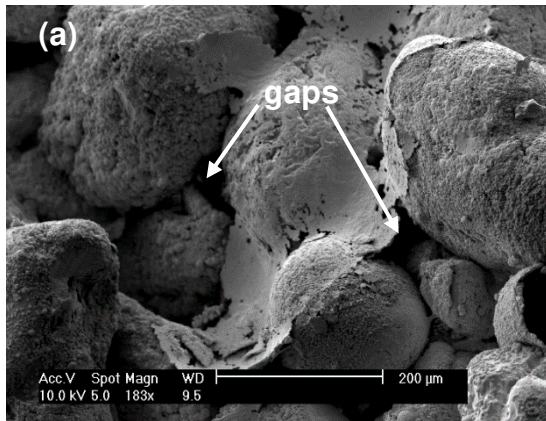
756



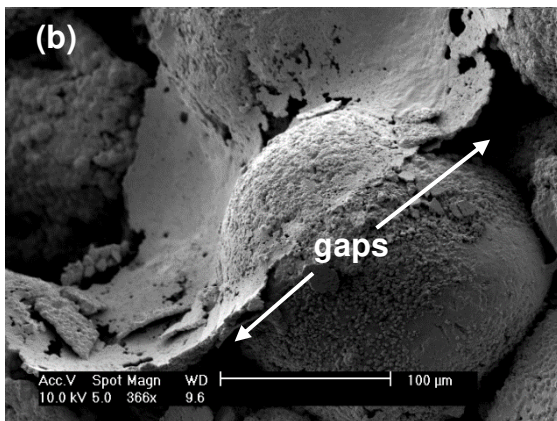
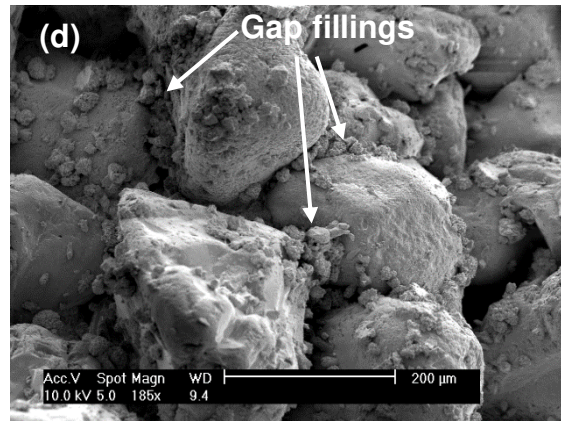
757

758

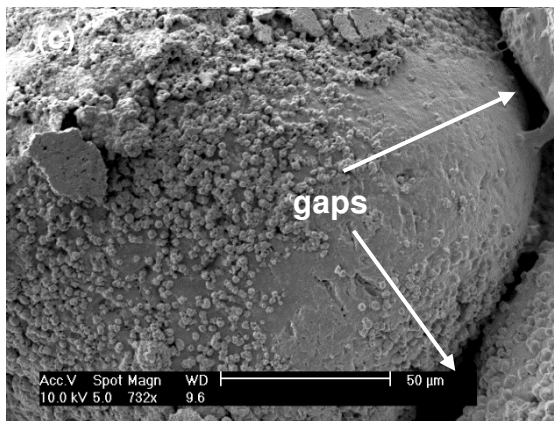
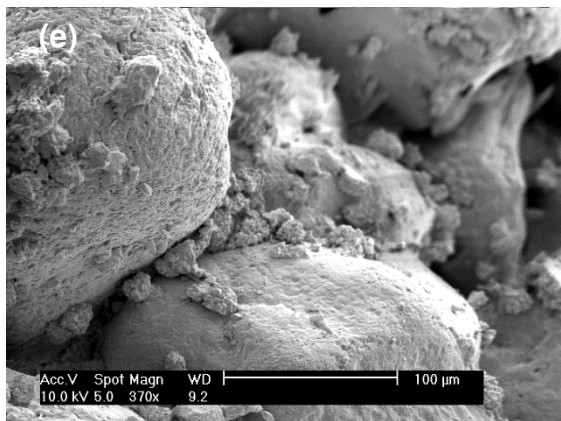
759 Fig. 2



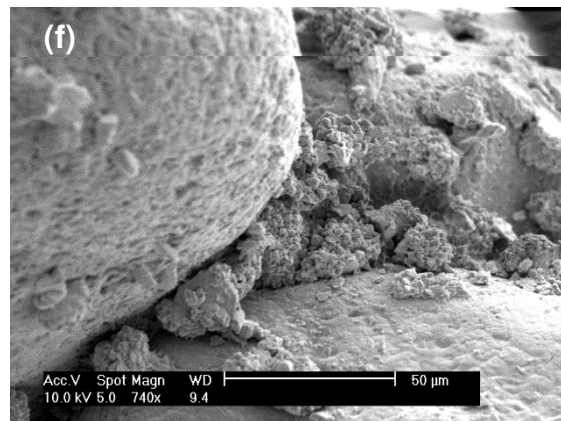
760



761



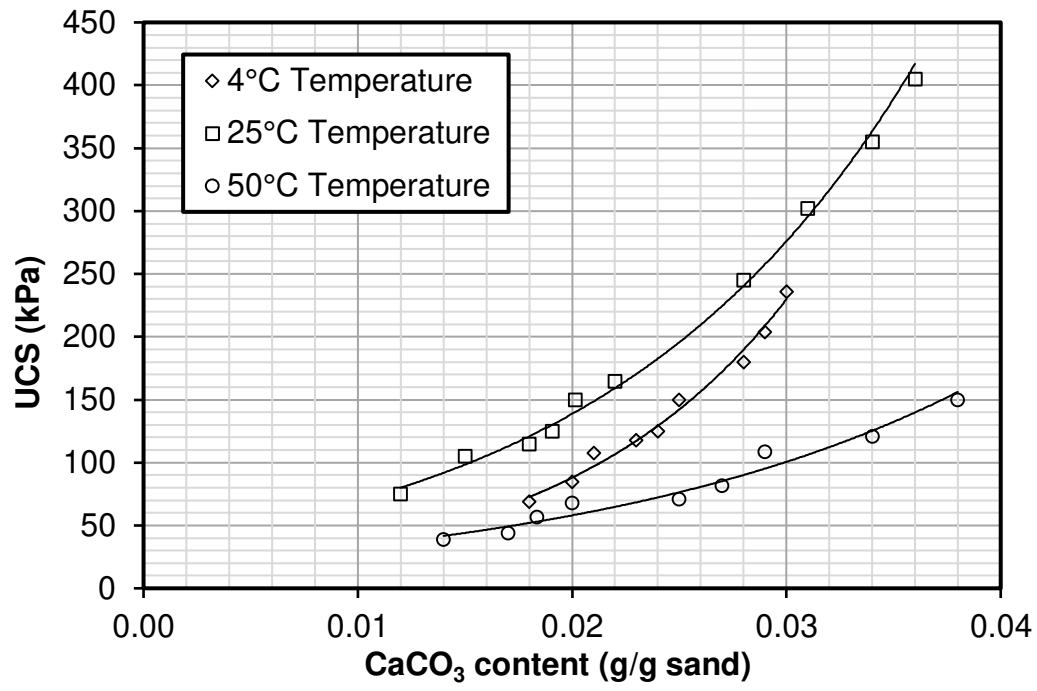
762



763

764

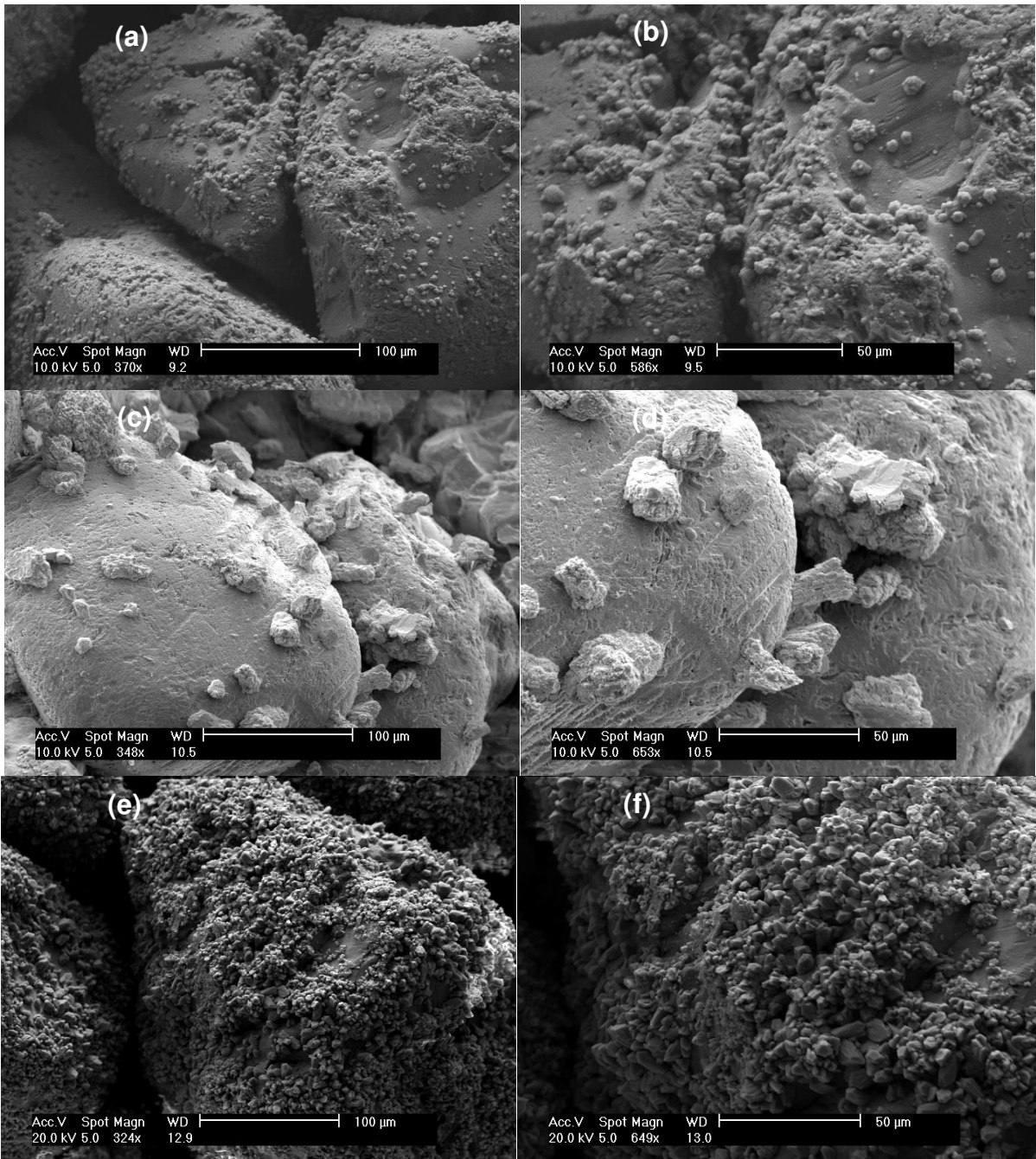
765 Fig. 3.



766

767

768 Fig. 4.
769



770

771

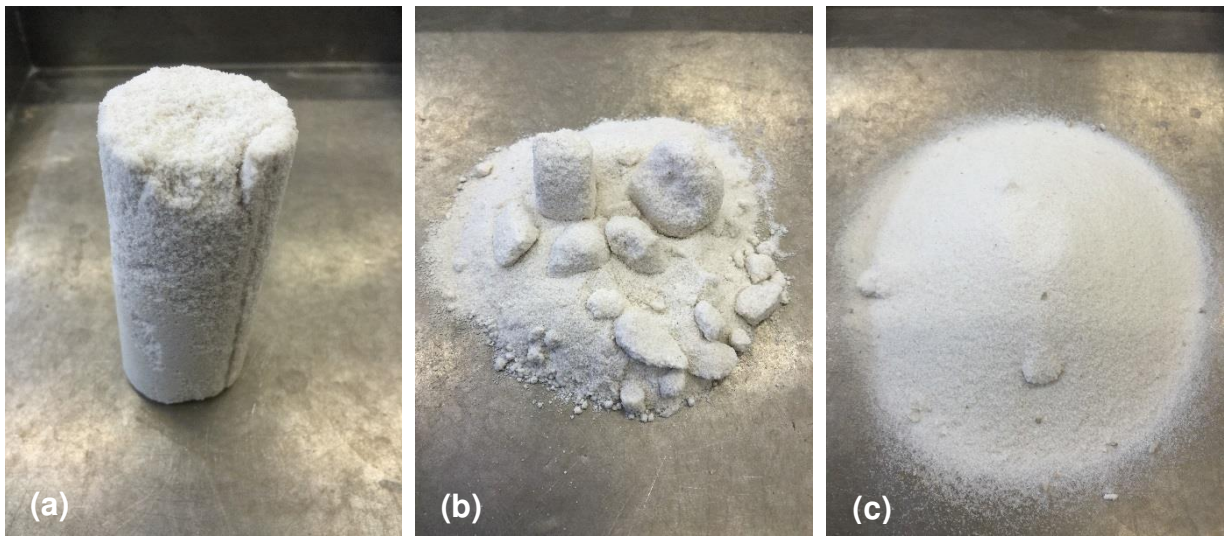
772

773

774

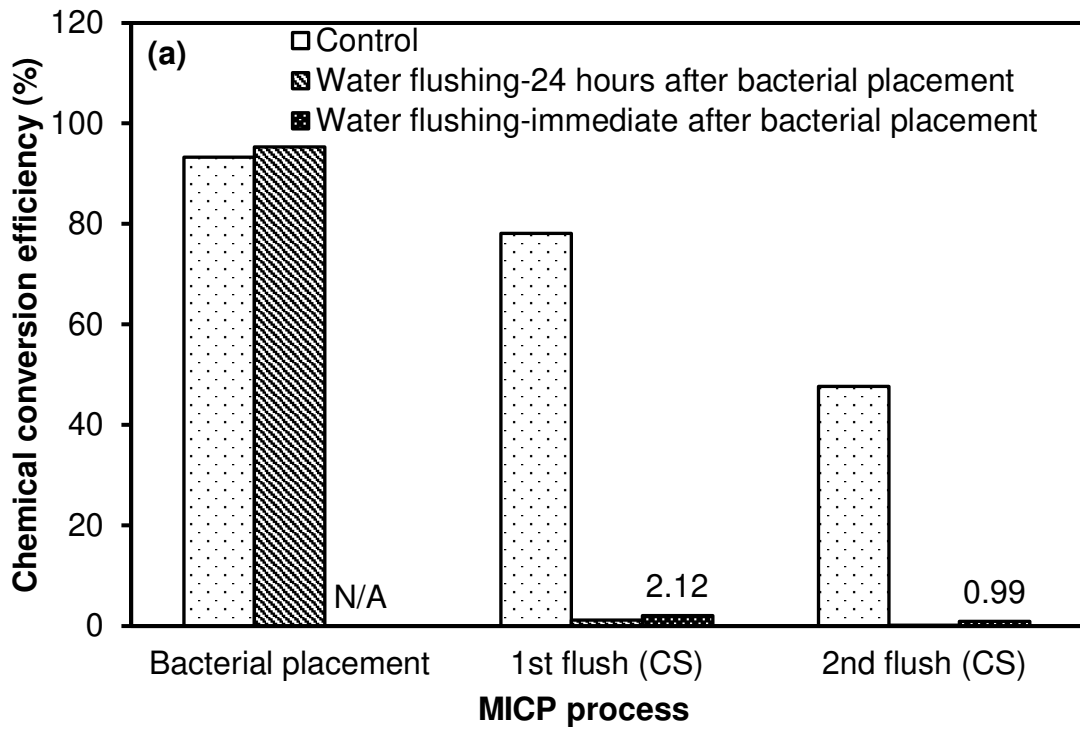
775

776 Fig. 5

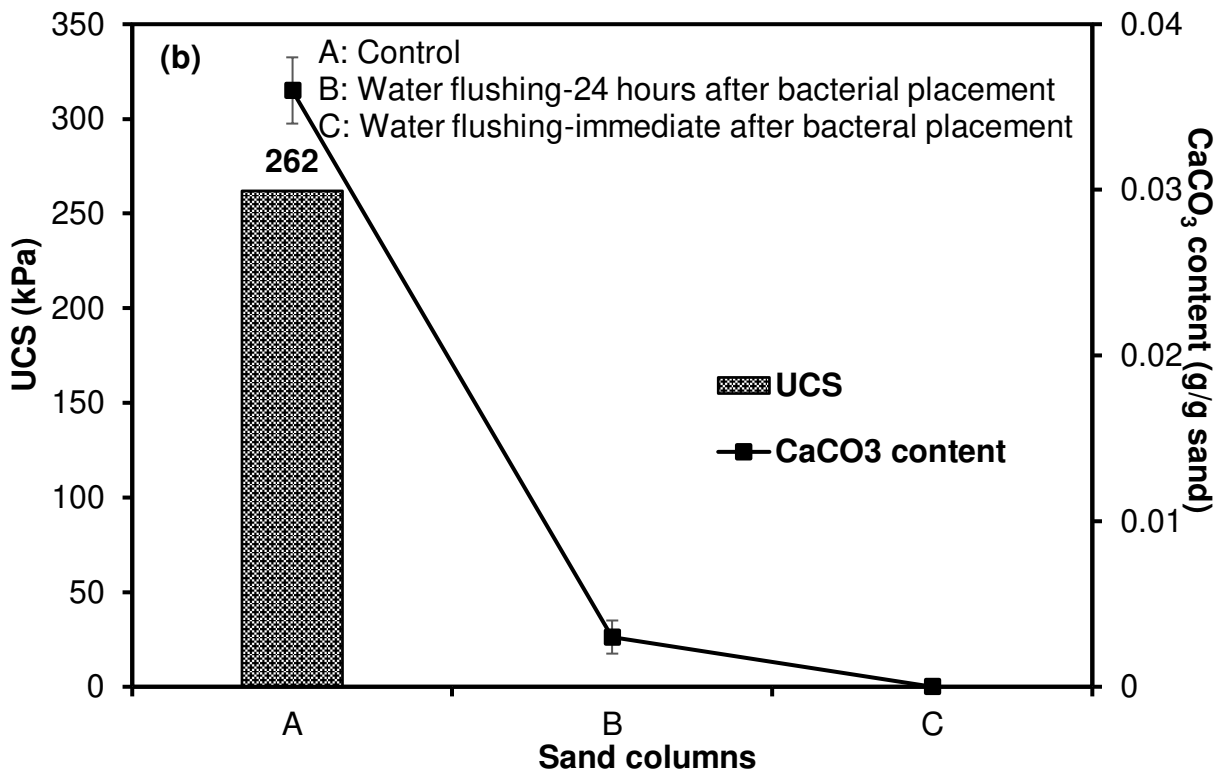


777

778 Fig. 6



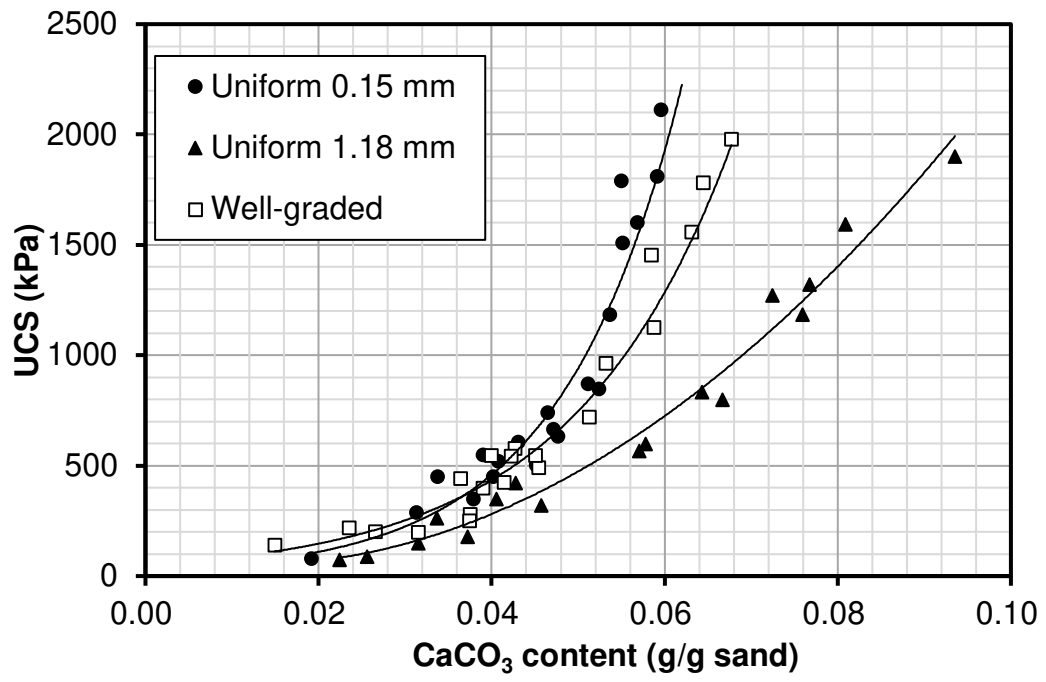
779



780

781

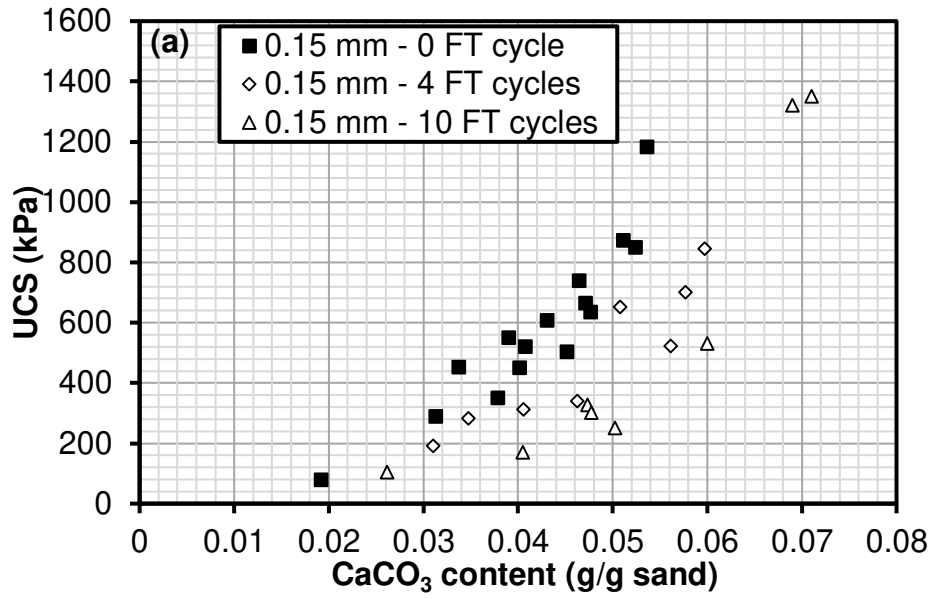
782 Fig. 7



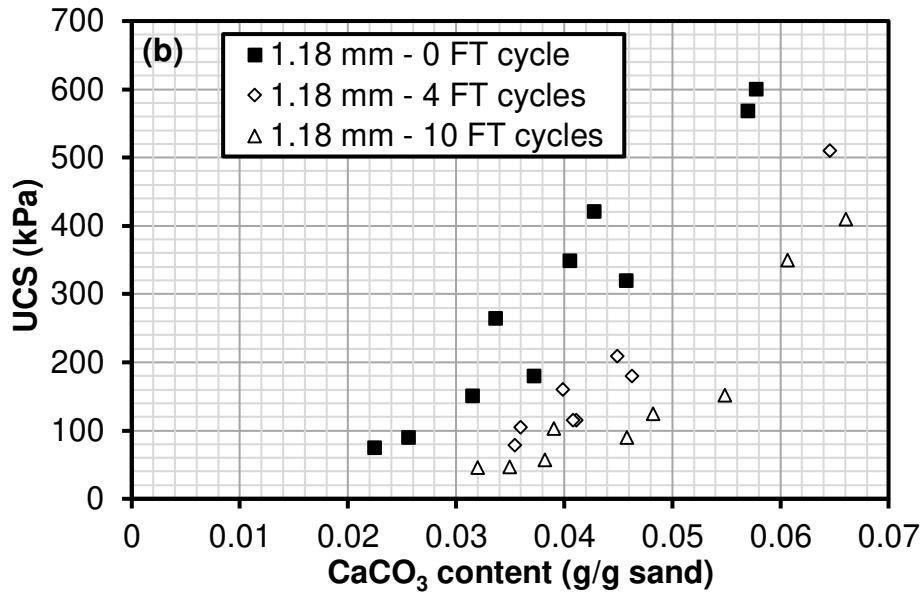
783

784

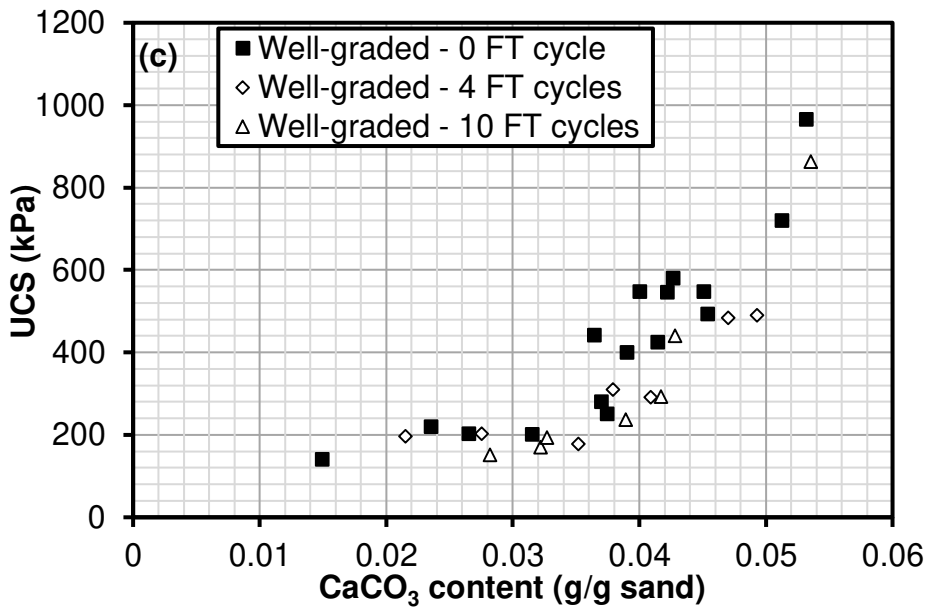
785 Fig. 8



786



787



788